REGULARIZATION DESIGN FOR BREAST LESION DETECTION IN PENALIZED MAXIMUM LIKELIHOOD IMAGE RECONSTRUCTION

Li Yang, Jian Zhou, Jinyi Qi

Department of Biomedical Engineering, University of California, Davis, CA, USA

ABSTRACT

Detecting cancerous lesion is a major clinical application in emission tomography. In a previous work, we have shown that penalized maximum likelihood image reconstruction can improve lesion detection at a fixed location by designing a shift-invariant quadratic penalty function. Here we extend this work to detection of tumors at unknown positions. We present a method to design a shift-variant quadratic penalty function that maximizes the detectability of lesions at all possible locations. We conducted computer-based Monte Carlo simulations to compare the optimized shift-variant penalty with the conventional penalty for detecting a breast lesion. Lesion detectability was assessed by a channelized Hotelling observer and human observer. The results showed a statistically significant improvement in lesion detection by using the optimized shift-variant penalty function compared to using the conventional penalty function.

Index Terms— Penalized likelihood reconstruction, lesion detection, PET, image quality

1. INTRODUCTION

Breast cancer is the most frequently diagnosed cancer in women. Early detection of breast cancer can increase the survival rate and treatment options. Although mammography has played a significant role in reducing breast cancer mortality, the accuracy of mammography is limited, especially in women with dense breasts. PET imaging has played a significant and evolving role in the staging, follow-up and management of metastatic breast cancer. However, current FDG-PET has low sensitivity to detect micrometastases and small tumor-infiltrated lymph nodes. Here we use the penalized maximum-likelihood (PML) reconstruction method to improve the detectability of small tumors in PET images by designing a penalty function specifically for lesion detection. Previously researchers have designed quadratic penalty function for uniform resolution [1] or maximimum contrast-to-noise ratio [2]. There is also a large body of literature developing edge-preserving priors, but we have not found any improvement in detection performance of lesions by using non-quadratic penalties [3]. In [4] we developed a method to design a quadratic penalty function to maximize the lesion detectability at a given location (e.g., the prostate). This paper extends this method to design a shift-variant penalty function for detecting lesions at unknown locations, which is more relevant to clinical PET applications where we do not know the lesion location *a priori*.

One advantage of the proposed penalty design is that the penalty function is patient-specific because it can take into account of the noise statistics of the emission data. However, this also requires the design procedure to be fast so that it can be applied in real clinical imaging. The basic theory and methods to address the computational challenges will be described in the next section.

This work was supported Grant Number R01EB000194 from the National Institute Of Biomedical Imaging And Bioengineering.

2. METHOD

2.1. System model and image reconstruction

In emission tomography, the measured sinogram data, $\boldsymbol{y} \in \mathbb{R}^{M\times 1}$, can be modeled as a collection of independent Poisson random variables with the expectation, $\bar{\boldsymbol{y}} \in \mathbb{R}^{M\times 1}$, related to the unknown tracer distribution, $\boldsymbol{x} \in \mathbb{R}^{N\times 1}$, through an affine transformation

$$\bar{\boldsymbol{y}} \equiv E[\boldsymbol{y}|\boldsymbol{x}] = \boldsymbol{P}\boldsymbol{x} + \boldsymbol{r}, \tag{1}$$

where $\boldsymbol{P} \in \mathbb{R}^{M\times N}$ is the detection probability matrix with the (i,j)th element equal to the probability of detecting an event from the jth voxel at the ith line of response, and $\boldsymbol{r} \in \mathbb{R}^{M\times 1}$ is the expectation of the background events (scattered and random events) in the data. The log likelihood function is given by

$$L(\boldsymbol{y}|\boldsymbol{x}) = \sum_i (y_i \log \bar{y}_i - \bar{y}_i - \log y_i!). \tag{2}$$

Penalized likelihood methods regularize the image through the use of a roughness penalty function. The quadratic penalty function can be expressed as

$$\phi(\boldsymbol{x}) = \frac{1}{2}\boldsymbol{x}'\boldsymbol{R}\boldsymbol{x}, \tag{3}$$

where $\boldsymbol{R}$ is a positive semi-definite matrix and $'$ denotes vector (or matrix) transpose. Combining the likelihood function

and the penalty function, the PML solution is found as

$$\hat{\boldsymbol{x}}(\boldsymbol{y}) = \arg\max_{\boldsymbol{x}\geq 0}[L(\boldsymbol{y}|\boldsymbol{x}) - \beta\phi(\boldsymbol{x})], \tag{4}$$

where β is a parameter that controls the degree of regularization.

2.2. Lesion detection analysis

To study lesion detectability, channelized Hoteling observers (CHOs) [5] is used here because many studies have shown that CHOs have good correlation with human performance. The test statistic of the CHO is

$$\eta_{\mathrm{CHO}}(\hat{\boldsymbol{x}}) = \boldsymbol{z}'\boldsymbol{U}'\boldsymbol{K}^{-1}(\boldsymbol{U}\hat{\boldsymbol{x}} + \boldsymbol{n}) \tag{5}$$

where $\boldsymbol{z}$ is the expected profile of the reconstructed lesion, i.e., $\boldsymbol{z} = E[\hat{\boldsymbol{x}}|H_1] - E[\hat{\boldsymbol{x}}|H_0]$ (H_0 is the null hypothesis representing lesion absent and H_1 is the alternative hypothesis representing lesion present), $\boldsymbol{U}$ denotes a set of frequency-selective channels, $\boldsymbol{n}$ is the internal channel noise that models the uncertainty in human detection process with mean zero and covariance $\boldsymbol{K}_N$ [5]. $\boldsymbol{K}$ is the covariance of the channel outputs and can be computed by

$$\boldsymbol{K} = \frac{1}{2}\boldsymbol{U}(\boldsymbol{\Sigma}_{\hat{\boldsymbol{x}}|H_1} + \boldsymbol{\Sigma}_{\hat{\boldsymbol{x}}|H_0})\boldsymbol{U}' + \boldsymbol{K}_N, \tag{6}$$

where $\boldsymbol{\Sigma}_{\hat{\boldsymbol{x}}|H_1}$ and $\boldsymbol{\Sigma}_{\hat{\boldsymbol{x}}|H_0}$ are the covariance matrices of $\hat{\boldsymbol{x}}$ under hypotheses of H_1 and H_0, respectively.

The detection performance can be measured by the SNR of $\eta(\hat{\boldsymbol{x}})$, which is defined as

$$\mathrm{SNR}^2[\eta(\hat{\boldsymbol{x}})] = \frac{(E[\eta(\hat{\boldsymbol{x}})|H_1] - E[\eta(\hat{\boldsymbol{x}})|H_0])^2}{(\mathrm{var}[\eta(\hat{\boldsymbol{x}})|H_1] + \mathrm{var}[\eta(\hat{\boldsymbol{x}})|H_0])/2}. \tag{7}$$

Using the results derived in [6], the SNR of CHO can be approximated by

$$\mathrm{SNR}^2_{\mathrm{CHO}} \approx \bar{\boldsymbol{f}}_l'\boldsymbol{F}[\boldsymbol{F} + \beta\boldsymbol{R}]^{-1}\boldsymbol{U}'\boldsymbol{K}^{-1}\boldsymbol{U}[\boldsymbol{F} + \beta\boldsymbol{R}]^{-1}\boldsymbol{F}\bar{\boldsymbol{f}}_l \tag{8}$$

where

$$\boldsymbol{K} \approx \boldsymbol{U}[\boldsymbol{F} + \beta\boldsymbol{R}]^{-1}\boldsymbol{F}[\boldsymbol{F} + \beta\boldsymbol{R}]^{-1}\boldsymbol{U}' + \boldsymbol{K}_N, \tag{9}$$

and $\bar{\boldsymbol{f}}_l \equiv E[\boldsymbol{x}|H_1] - E[\boldsymbol{x}|H_0]$ is the expectation of the lesion profile, $\boldsymbol{F} = \boldsymbol{P}'\mathrm{diag}[\frac{1}{\bar{\boldsymbol{y}}}]\boldsymbol{P}$ is the Fisher information matrix, and $\bar{\boldsymbol{y}} \equiv \boldsymbol{P}\{E[\boldsymbol{x}|H_1] + E[\boldsymbol{x}|H_0]\}/2 + \boldsymbol{r}$.

For fast computation, we approximate $\boldsymbol{F}$ and $\boldsymbol{R}$ locally using circulant matrices $\hat{\boldsymbol{F}}$ and $\hat{\boldsymbol{R}}$, respectively, based on the observation that $\boldsymbol{F}$ and $\boldsymbol{R}$ vary smoothly in space. $\hat{\boldsymbol{F}}$ and $\hat{\boldsymbol{R}}$ are constructed using the column vectors of $\boldsymbol{F}$ and $\boldsymbol{R}$ corresponding to the voxel at the center of lesion, respectively. Because circulant matrices can be diagonalized by Fourier transform, we can evaluate (8) quickly using the fast Fourier transform as

$$\mathrm{SNR}^2_{\mathrm{CHO}} \approx \left[\sum_i \frac{\tilde{U}_{k,i}\lambda_i\xi_i}{\lambda_i + \beta\mu_i}\right]' \boldsymbol{K}^{-1} \left[\sum_i \frac{\tilde{U}_{k,i}\lambda_i\xi_i}{\lambda_i + \beta\mu_i}\right] \tag{10}$$

where

$$\boldsymbol{K} \approx \tilde{\boldsymbol{U}}\mathrm{diag}\left[\frac{\lambda_i}{(\lambda_i + \beta\mu_i)^2}\right]\tilde{\boldsymbol{U}}' + \boldsymbol{K}_N. \tag{11}$$

Here $\tilde{\boldsymbol{U}}$ are the Fourier coefficients of the channel functions, $\{\xi_i,\ i = 1, ..., N\}$ is the Fourier transform of $\bar{f}_l$, and $\{\lambda_i,\ i = 1, ..., N\}$ and $\{\mu_i,\ i = 1, ..., N\}$ are the eigenvalues (Fourier coefficients) of $\hat{\boldsymbol{F}}$ and $\hat{\boldsymbol{R}}$, respectively. Details can be found in [6].

2.3. Regularization design

For a given dataset, equation (10) can be used to evaluate lesion detectability under different regularization parameters and to guide penalty design. We decompose the quadratic penalty function in (3) into pairwise penalties in the following form

$$\boldsymbol{x}'\boldsymbol{R}\boldsymbol{x} = \sum_{j=1}^{N}\sum_{l\in\mathcal{N}_j}\gamma_{jl}(x_j - x_l)^2 \tag{12}$$

where $\mathcal{N}_j$ denotes the neighborhood of the jth pixel and γ_{jl} is the weighting factor for the pairwise penalty. Then the design of the penalty function becomes finding $\{\gamma_{jl}\}$ that maximize the lesion detectability. In the previous work [4], the lesion detectability was evaluated at a fixed position and the weighting factors were kept spatially invariant, i.e., γ_{jl} is only a function of $j-l$. For detecting lesions at unknown locations, here we calculate the weighting factors γ_{jl} for every pixel j and form a shift variant matrix $\boldsymbol{R}$. To enforce the symmetry of $\boldsymbol{R}$, the final penalty function is computed as

$$\boldsymbol{x}'\boldsymbol{R}\boldsymbol{x} = \sum_{j=1}^{N}\sum_{l\in\mathcal{N}_j}\frac{\gamma_{jl} + \gamma_{lj}}{2}(x_j - x_l)^2. \tag{13}$$

One constraint on the weighting factors is that the resulting $\boldsymbol{R}$ should be positive semi-definite, which can be satisfied by constraining all γ_{jl} to be non-negative. Although $\gamma_{jl} \geq 0$ is a sufficient, but not necessary, condition, we found little improvement in CHO SNR by allowing γ_{jl} to take negative values in our experiments. The penalty design thus reduces to compute the optimal weighting factors at each pixel j by

$$\{\gamma_{jl}\} = \arg\max_{\gamma_{jl}\geq 0}\mathrm{SNR}^2_{\mathrm{CHO}}. \tag{14}$$

Performing the optimization in (14) for every pixel is time-consuming. To reduce the computation cost, we only compute the optimum weighting factors on a coarse grid and then

assign the values of γ_{jl} to other pixels using the nearest neighbor interpolation. We found that γ_{jl} varies slowly as we move from one pixel to its neighbors, so this interpolation method works well. The number of pixels on the coarse grid was determined experimentally.

3. SIMULATION RESULT

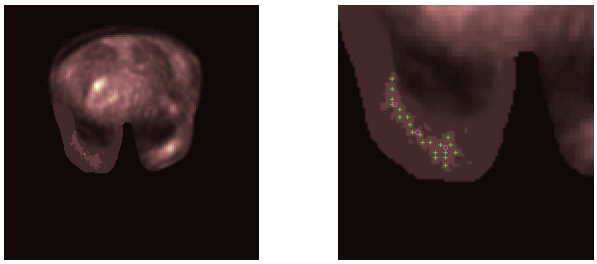
3.1. Computer simulations

We simulated a 2D PET system, which has same parameters as a GE DST clinical scanner. The digital phantom was created based on a patient PET/CT scan, where there was a histologically verified tumor in the left breast. Currently PET imaging of breast cancer is often used to detect distant metastases for staging purpose. Thus we simulated detection of a small tumor in the contralateral breast. We segmented the fat tissue and glandular tissue in the contralateral breast and assigned a uniform activity to each tissue type based on the original PET image.

A small lesion was simulated as a round hot spot with a diameter of 3 mm and contrast of 5:1. To evaluate the proposed penalty design method for detecting a tumor at unknown positions, we inserted the lesion at three different locations in the glandular tissue. Figure 1(a) shows the phantom image with the simulated lesion at one possible location. All three lesion locations are indicated by the purple "o" marks in Fig. 1(b). For each lesion location, the phantom images with and without a lesion were forward projected to generate noisefree projections. Independent Poisson noise was then added to the noisefree sinogram to generate 600 independent realizations with the expected total number of events equal to one million.

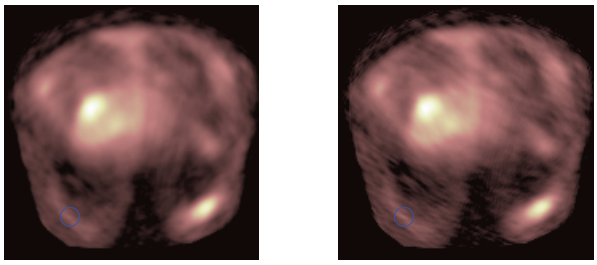
To compute the shift variant penalty matrix $\boldsymbol{R}$, we used a CHO with three difference-of-Gaussian channels and white Gaussian internal noise (mean zero and standard deviation equal to 5.6% of the mean glandular tissue activity). We computed the optimal weighting factor γ_{jl} based on equation (14) at 21 selected locations in the glandular tissue (represented by the green "+" marks in Fig. 1(b)). The neiborhood $\mathcal{N}_j$ was chosen to include 20 nearest pixels. Because of the symmetry, only ten independent γ_{jl}'s need to be determined for each pixel. The weights at all other pixels were assigned based on its nearest neighbor in the 21 samples. The proposed penalty matrix $\boldsymbol{R}$ was then formed by equation (13). To examine the effect of the nearest neighbor interpolation, we computed the maximal SNR for all the 21 selected locations using γ_{jl} computed at its own position and the one from its nearest neighbor in the set. The resultant difference between the maximal SNR values was less than 0.2%, which suggests that the effect of the interpolation is negligible.

To verify the lesion detectability in reconstructed images, we reconstructed all the datasets using both the proposed penalty and the conventional first-order quadratic penalty. The images were reconstructed using a MAP EM algorithm with



(a) (b)

Fig. 1. (a) The digital PET phantom with a simulated 3-mm lesion. (b) A zoom-in image of the contralateral breast with the green "+"s indicating the 21 sample points for calculating γ_{jl} and purple "o"s depicting the three lesion locations.



(a) (b)

Fig. 2. Sample reconstructed images with a 3-mm lesion at the center of the blue circle using (a) the conventional first-order penalty function and (b) the proposed penalty function.

256×256 3-mm square pixels. The weighting factors γ_{jl} in both penalty functions were scaled so that the detectability of the lesion is maximized at $\beta = 1$ as predicted by (10). Sample reconstructed images are shown in Fig. 2. Although the image reconstructed using proposed penalty shows more streaks than the one using conventional penalty, it does not affect the lesion detectability in the SKE/BKE task. To compare the lesion detectabilities quantitatively, we plot the SNR of the CHO as a function of β in Fig. 3 (left column). The Monte Carlo SNR was computed from the 600 independently reconstructed images under each condition. The standard deviation of each Monte Carlo SNR was estimated using a bootstrap method. In general, the Monte Carlo results match the theoretical predictions very well. Both Monte Carlo and theoretical results show that the proposed penalty function improves lesion detectability compared to the conventional penalty by around 10% for all the three locations.

3.2. Human observer study

We performed a human observer study to verify the numerical observer results. A human observer is asked to perform a two-alternative force-choice (2AFC) experiment for each lesion

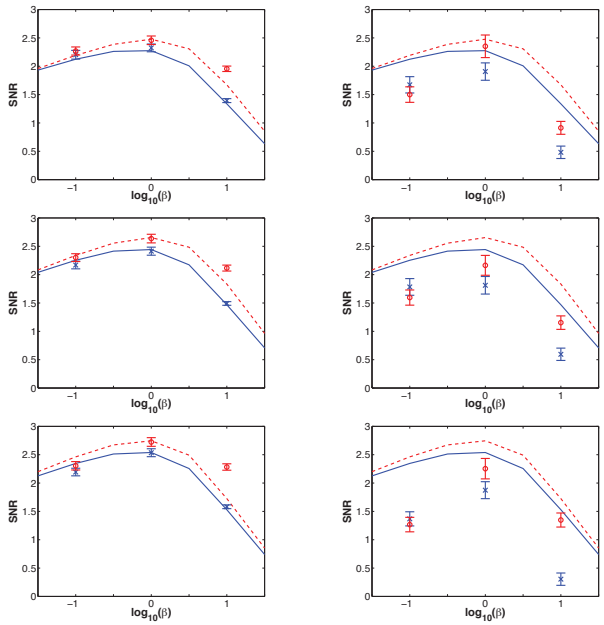


Fig. 3. Comparison of the Monte Carlo results (left column) and human observer study (right column) with the theoretical predications using the conventional penalty (blue solid line) and proposed penalty (red dash line) for the three lesion locations: the uppermost position (top row), middle position (middle row), lowermost position (bottom row). The Monte Carlo and human observer results of the conventional penalty are marked by "×" and those of the proposed penalty by "o". The error bars indicate plus and minus one standard deviation.

location. The resulting percent correct (PC) in the 2AFC test [7] was converted to the SNR by,

$$\mathrm{SNR} = 2\mathrm{erf}^{-1}(2\mathrm{PC} - 1). \tag{15}$$

The results (Fig. 3 right column) show that the detection performance of the human observer follow the same trends as the theoretical predictions. The difference in the detectability between the human observer and the theoretical prediction may be caused by the nonspecific CHO model, which indicates a well-designed observer-specific CHO model can be helpful. Since the theoretical results do not rely on the particular choice of the channel parameters, it can be applied to other channel parameters.

We performed a binomial test on the human observer 2AFC results at the optimal β for all three lesion locations. Each 2AFC experiment was considered as a Bernoulli experiment with two possible outcomes (0 for incorrect choice and 1 for correct choice) with a success probability equal to the PC. The outcomes of the 2AFC experiments for each lesion location can be sorted into four categories with probabilities shown in table 1, where P_1 denotes the PC under the conventional first-order penalty, and P_p denotes the PC under the proposed penalty. Under the null hypothesis that there is no difference between the two PCs ($P_1 = P_p$), categories 3 and 4 should happen with the same probability ($N_3 \approx N_4$). From the observed values of N_3 and N_4, we obtained a p-value of 2.84×10^{-6}, which shows that the improvement in lesion detection by the proposed penalty is statistically significant.

Table 1. Four categories of the 2AFC experiment outcomes under the conventional penalty and the proposed penalty.

	1st order penalty	Proposed penalty	Probability	Number of cases
1	1	1	P_1P_p	N_1
2	0	0	$(1-P_1)(1-P_p)$	N_2
3	1	0	$P_1(1-P_p)$	N_3
4	0	1	$(1-P_1)P_p$	N_4

4. CONCLUSION

We have developed a method to design the quadratic penalty function in PML image reconstruction for lesion detection at a unknown location. Using computer simulations and human observer study we have evaluated the proposed method for detecting a hot lesion in a breast phantom. The results show that the proposed method can significantly improve the lesion detectability over the conventional quadratic penalty function. In future work, we plan to extend the current model to 3D and to evaluate our method using real patient data.

5. REFERENCES

[1] J.W. Stayman and J.A. Fessler, "Regularization for uniform spatial resolution properties in penalized-likelihood image reconstruction," *IEEE Trans. Med. Imag.*, vol. 19, no. 6, pp. 601–15, June 2000.

[2] J. Qi and R.M. Leahy, "A theoretical study of the contrast recovery and variance of MAP reconstructions from PET data," *IEEE Trans. Med. Imag.*, vol. 18, no. 4, pp. 293–305, Apr. 1999.

[3] J. Qi, "Investigation of Lesion Detection in MAP Reconstruction with Non-Gaussian Priors," in *Proc. IEEE Nucl. Sci. Symp.*, 2005, vol. 3, pp. 1704–1708.

[4] J. Qi and R.H. Huesman, "Penalized maximum likelihood image reconstruction for lesion detection," *Phys. Med. Biol.*, vol. 51, no. 16, pp. 4017–29, Aug. 2006.

[5] J. Yao and H.H. Barrett, "Predicting human performance by a channelized hotelling model," in *Proc. SPIE*, 1992, vol. 1768, pp. 161–168.

[6] J. Qi, "Analysis of lesion detectability in Bayesian emission reconstruction with nonstationary object variability," *IEEE Trans. Med. Imag.*, vol. 23, no. 3, pp. 321–9, Mar. 2004.

[7] A.E. Burgess, "Comparison of receiver operating characteristic and forced choice observer performance measurement methods," *Med. Phys.*, vol. 22, no. 5, pp. 643–55, May 1995.